JOURNAL OF MATERIALS SCIENCE 37 (2002) 185–190

Effect of composition and thermal cycling on the adhesion strength of Sn-Zn-Al solder hot-dipped on Cu substrate

SHAN-PU YU
Department of Materials Science and Engineering, National Cheng Kung University, 1 Ta Hsueh Road, Tainan, 70101, Taiwan

HSIN-CHIEN WANG, MOO-CHIN WANG
Department of Mechanical Engineering, National Kaohsiung Institute of Technology, 415 Chien-Kung Road, Kaohsiung, 80782, Taiwan

MIN-HSIUNG HON
Department of Materials Science and Engineering, National Cheng Kung University, 1 Ta Hsueh Road, Tainan, 70101, Taiwan

Reliability losses in many electronic systems were identified with the failure of solder joints rather than device malfunctions. The adhesion strength is an important factor for assessing the reliability of the solder joints. In this work, a pull-off test was used to investigate the adhesion strength at the interface of the $(100-x)$Sn-x(5Al-Zn) lead-free solders on Cu substrate as-soldered and after thermal cycling, respectively. For the $(100-x)$Sn-x(5Al-Zn) solders with the x value increased up to 40 wt%, the adhesion strength decreased from 11.8 ± 1.5 to 3.3 ± 0.9 MPa. After thermal cycling (-20–120°C) for 40 cycles, the adhesion strength of 95Sn-5(5Al-Zn) and 91Sn-9(5Al-Zn) solders decreased from 11.2 ± 1.7 to 8.2 ± 1.3, 7.6 ± 0.7 to 5.0 ± 0.8 MPa, respectively. However, the adhesion strength for the solders of 80Sn-20(5Al-Zn), 70Sn-30(5Al-Zn) and 60Sn-40(5Al-Zn) increased from 5.7 ± 1.7 to 13.3 ± 1.9 MPa, 4.8 ± 2.0 to 12.2 ± 1.8 MPa, and 3.3 ± 1.5 to 16.2 ± 1.2 MPa, respectively. The formation of intermetallic compound (IMC) is proposed for the enhancement of the strength after thermal cycling in this study.

1. Introduction

Solder joints serve as connections in package and influence the signal and power distribution, heat dissipation, and mechanical support and productions [1, 2]. In addition, it also plays an important role in today's surface mount technology (SMT) high density package due to the smaller contact area. The reliability of solder joints has thus been regarded as the most critical issue in SMT because of large strains developed at the interconnection between the components and the substrate material during operation. The strains may cause severe cracking and premature failure in the solder joints. Besides, the stress concentration, the intermetallics formed at the solder/substrate interface are also another causes for the failure of solder joints [3].

A key issue in the long-term reliability of solder joints is the failure during thermal cycling. During soldering, the adhesion of solder to substrate is thought to be beneficial since the solder is viewed as a compliant member and would take up the strain without damage. However, due to the effect of thermal cycling on the solder joint during the on off of power switch, the residual stress upon the solder and the interface of solder/substrate increases [4–6]. Under thermal cycles, mechanical deformation can occur at solder joints due to thermomechanical fatigue (e.g., environmental-temperature cycles on joined materials with different coefficients of thermal expansion). Moreover, mechanical deformation occurs during shipping, dropping of the electronics, or device assembly [7].

For various kinds of materials used in the joint assembly, the fracture behaviors under the mechanical test for the solder/substrate joint assembly after aged or thermal cycling have often revealed a scattering of fracture modes at the interface. It is due to the variation of the microstructure of the solder/substrate interface. The formation of IMC as soldering and its behaviors as thermal cycling are thought to be the major causes.

The adhesion strength and fracture mode of Sn-Zn-Al solder alloys with various 5Al-Zn contents after thermal cycling were investigated in this work.

2. Experimental procedures

2.1. Sample preparation

The Sn-Zn-Al solders were prepared by melting the 5Al-Zn master alloy with Sn. Accordingly, the solder compositions are $(100-x)$Sn-x(5Al-Zn) wherein

0022–2461

$(100 - x)$ and x represents the weight percentage of Sn and 5Al-Zn, respectively.

The substrate of Cu plate (about 99.9% pure), approximately 65 mm × 20 mm × 2.5 mm was degreased in an alkaline solution of NaOH (5 wt%) for 15 s, followed by rinsing in de-ionized (DI) water for 10 s. The copper substrate was then pickled in HCl solution (5 vol%) for 10 s, followed by rinsing in DI water again. The substrate was dipped in a dimethylammonium chloride (DMAHCl) flux (2.5 g DMAHCl/100 cc C_2H_5OH) for 10 s after the pretreatment mentioned above. After being fluxed, the sample was immersed in an Sn-Zn-Al solder bath at 300°C ($x = 5$,9), 350°C ($x = 20$,30) and 400°C ($x = 40$) respectively for 10 s.

2.2. Thermal cycling test

Thermal cycling was carried out in air from −20°C (10 min) to 120°C (10 min). A schematic diagram of the thermal cycling profile is shown in Fig. 1.

2.3. Adhesion strength measurement

The adhesion strength was measured with a pull-off tester. The surface of samples was ground with No. 1500 sand paper to smooth the surface of hot-dipped solder film and achieved a 10 μm thick solder layer, and then cleaned in acetone. The smooth surface of these samples was adhered to an aluminum stud using epoxy followed by a cure at 150°C for 1 h. The diameter of studs was 2.69 mm (0.106 in), and the strength of the epoxy was about 70 MPa. The force was applied to the stud at a rate of 9.06 kgf/s for the pull-off test. The apparatus stopped applying force when the stud separated from the sample. The adhesion strength, ratio of the fracture force divided by the area of stud, was calculated by a computer. Ten experiments of adhesion strength measurement were conducted for each condition studied.

2.4. Microstructure analyses

The fractured and cross-sectional microstructures of sample prepared by standard metallographic process were observed by scanning electron microscopy (SEM). The energy dispersion spectroscopy (EDS) was used for element quantitative analysis.

3. Results and discussion

3.1. Composition effect

Yu *et al*. [8] reported that the primarily solidified phase consists greater contents of Al and Zn (Al, Zn-rich), while the secondarily solidified phase is with less contents of Al and Zn (Sn-rich). This is reasonable as the phase with greater contents of high melting temperature elements of Al and Zn is expected to solidify first. When the x value was increased, the morphology of primarily solidified phase changed from spherical to needle-like lamella eutectic microstructure for $x = 5$ and 20, while a larger cluster was formed for $x = 30$ and 40. The microstructure of the 60Sn-40(5Al-Zn) solder was similar to that of the 70Sn-30(5Al-Zn) solder, except that more fractions of primary phase were found [8].

The adhesion strength of 91Sn-9Zn and $(100 - x)$ Sn-x(5Al-Zn) solders as shown in Fig. 2 indicates that the eutectic 91Sn-9Zn solders possess the highest adhesion strength of 11.8 ± 1.5 MPa. When x value of $(100 - x)$Sn-x(5Al-Zn) solders increased from 5 to 40, the adhesion strength decreased from 11.2 ± 0.5 to 3.3 ± 0.9 MPa while the thickness of IMC layer increased from less than 1 μm to about 2 μm as Yu *et al*. reported [8]. Table I lists the CTE of elements used in this study. Since the elements of Sn, Zn and Al all possess higher CTE values than Cu, especially Al and Zn, the micropores near Sn-rich/Al, Zn-rich, solder/IMC and solder/Cu interfaces would form and result in the decrease of adhesion strength for the as-solidified samples, especially for the solders with higher 5Al-Zn contents such as x values of 20, 30 and 40.

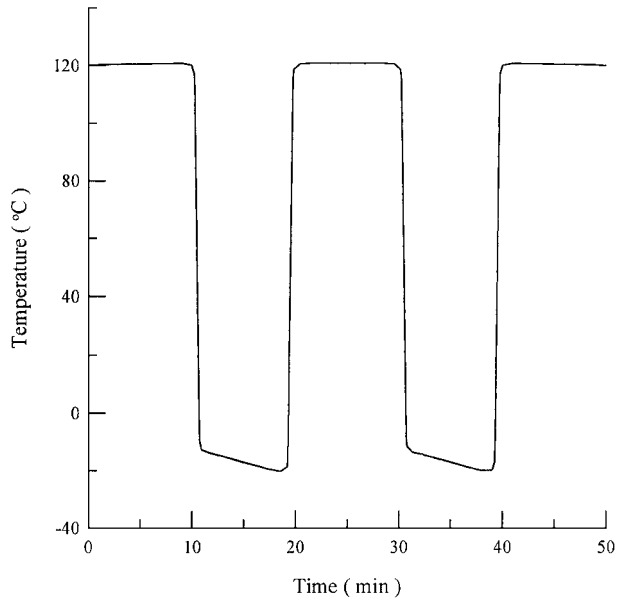

Figure 1 Schematic diagram of the thermal cycling profile.

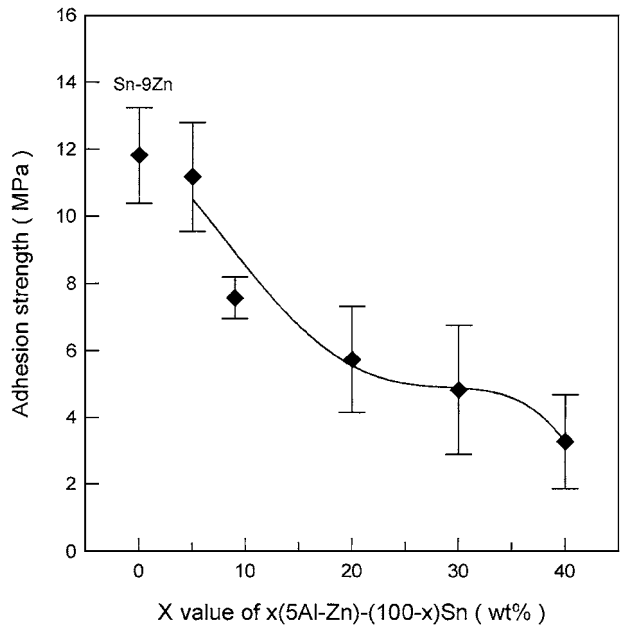

Figure 2 Adhesion strength of 91Sn-9Zn and $(100 - x)$Sn-x(5Al-Zn) solders with various x values.

TABLE I The coefficient of thermal expansion (CTE) of element used in this study [20]

Metal	CTE ($\times 10^{-6}$ /°C)
Cu	16.7
Sn	21
Zn	30
Al	23

Fig. 3 shows the SEM micrographs of as-dipped (a) 95Sn-5(5Al-Zn) and (b) 70Sn-30(5Al-Zn) solders after pull-off test. Fracture both occurred at solder bulk and solder/IMC interface for the samples shown in Fig. 3a and b. However, seldom IMC particle was found in 95Sn-5(5Al-Zn) solder while larger and more IMC particles were found for solder 70Sn-30(5Al-Zn). This phenomenon also illustrates that the adhesion strength decreased for the samples with thicker IMC layer such as hypereutectic Sn-Zn-Al alloys.

Interfacial phase transformation at the solder/substrate joint affects the IMC thickness significantly. The Cu_5Zn_8 IMC phase was found for the Sn-Zn-based solders such as Sn-Zn-Al [9, 10], Sn-Zn-In [11] and Sn-Zn [12] etc. Even Cu_9Al_4 was also found at Cu_5Zn_8/Cu interface [10]. The amount of 5Al-Zn affects the IMC thickness significantly. The formation of IMC weakened the bonding strength between solder and IMC. Not only the pores between the Sn-rich and Al, Zn-rich area were increased, but also between the IMC and solder as the 5Al-Zn contents increased up to 40 wt% [8].

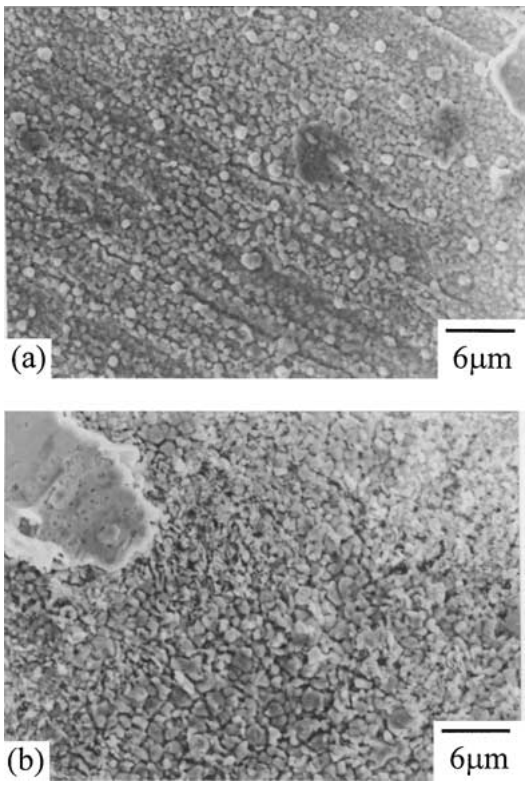

Figure 3 SEM micrographs of as-dipped (a) 95Sn-5(5Al-Zn) and (b) 70Sn-30(5Al-Zn) solder after pull-off test.

3.2. Thermal cycling effect

Thermal cycling is a key factor in simulating the use of electronic device under a severe temperature environment. In order to ensure the high reliability, it is inevitable to carry out the thermal cycling test of solder joint for practical integrated circuit (IC) devices.

Fig. 4a, b and c shows the adhesion strength of 91Sn-9Zn, 95Sn-5(5Al-Zn) and 91Sn-9(5Al-Zn) solders, respectively, which were hot-dipped on Cu substrate after various thermal cycles. In Fig. 3a, the adhesion strength of eutectic 91Sn-9Zn solder maintains a high value about 12 MPa while the thermal cycles were up to 40. However, the adhesion strength of 95Sn-5(5Al-Zn) solder decreased from 11.2 ± 1.7 to 8.2 ± 1.3 MPa as thermal cycles were up to 40 as shown in Fig. 4b. Simultaneously, the adhesion strength of the eutectic 91Sn-9(5Al-Zn) solder decreased from 7.6 ± 0.7 to 5.0 ± 0.8 MPa while thermal cycles were up to 40 as shown in Fig. 4c. These results are reasonable for most of the solder joints after thermal cycling test. The stress induced in solder joints during thermal cycling is mainly due to the thermal expansion mismatch of the different materials in a joint [13–19].

The adhesion strengths of solder $(100 - x)$Sn-x(5Al-Zn) with larger 5Al-Zn contents were shown in Fig. 5 with $x =$ (a) 20, (b) 30, and (c) 40, in which the adhesion strengths of the solders were increased from 5.7 ± 1.7 to 13.3 ± 1.9 MPa, 4.8 ± 2.0 to 12.2 ± 1.8 MPa, and 3.3 ± 1.5 to 16.2 ± 1.2 MPa for $x = 20$, 30 and 40, respectively, when thermal cycles were up to 40.

Fig. 6a and b shows the fracture surface of the 70Sn-30(5Al-Zn) sample after 40 thermal cycles, while Fig. 6c was the fracture surface of the Al stud site. Three different fracture layers were found in Fig. 6b in which the A region was the intermetallic/solder interface, while B region was the Al, Zn-rich cluster/solder interface, and the C region was the solder area. The B region appeared after thermal cycling in $(100 - x)$Sn-x(5Al-Zn) solder system with $x = 20$–40.

The weakest point in the joint layers determines the adhesion strength, which determines the solder joint reliability in actual applications. Frear *et al.* [3] reported that the cracks in thermal cycling experiments sometimes propagate through the intermetallics and the solder immediately adjoin to it. The weaker part of the two regions, solder or intermetallics, causes failures. The crack takes no definitive path while propagating to failure.

Fig. 7 shows the cross-sectional SEM micrographs of solder 70Sn-30(5Al-Zn) after 40 thermal cycles. Reacted band (A zone) between solder and Cu substrate was found at the interface between the Al, Zn-rich area (B zone, dark area) and Cu substrate, while C zone was the Sn-rich area near A or B zone. The EDS analyses of A and B areas in Fig. 7 shown in Fig. 8a and b, respectively, indicate that A was an Al, Zn-rich zone from the excessive 5Al-Zn contents in 70Sn-30(5Al-Zn) solders comparing to the eutectic 91Sn-9(5Al-Zn). However, the reacted band (A area), close to Cu substrate, was an IMC layer with higher Zn and Cu contents but a few Al dissolved-in after several thermal cycles as identified by EDS in Fig. 8a. The adhesion strength

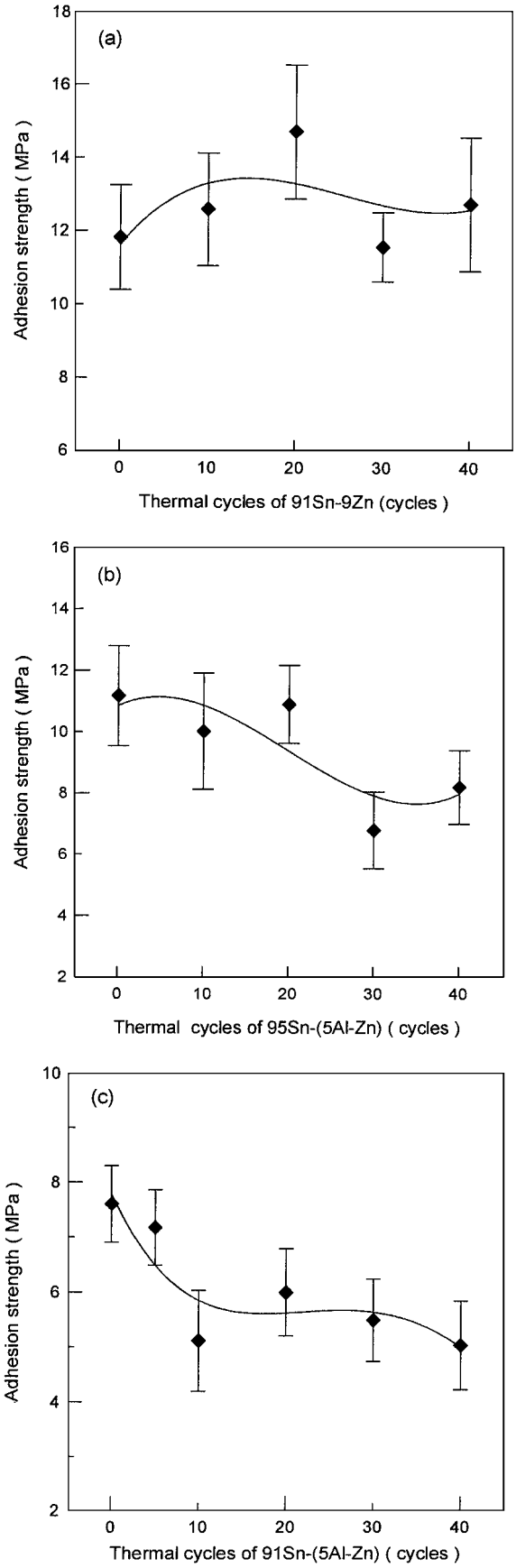

Figure 4 Adhesion strength of (a) 91Sn-9Zn, (b) 95Sn-5(5Al-Zn) and (c) 91Sn-9(5Al-Zn) solders hot-dipped on Cu substrate after various thermal cycles.

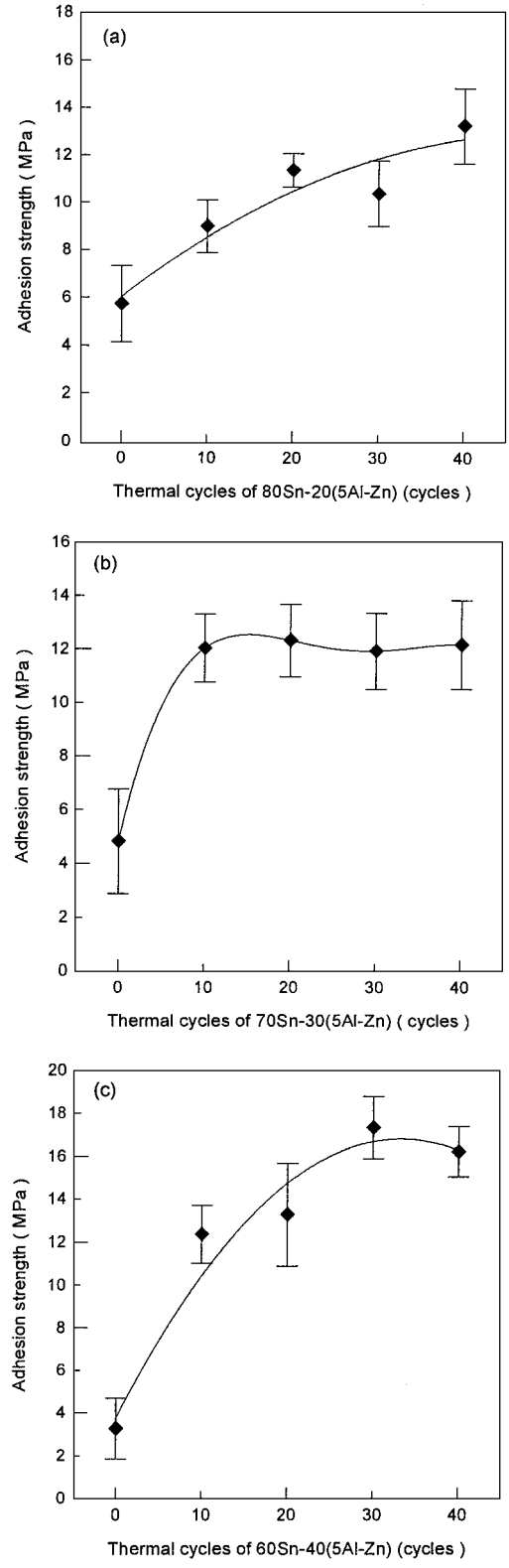

Figure 5 Adhesion strength of (a) 80Sn-20(5Al-Zn), (b) 70Sn-30(5Al-Zn) and (c) 60Sn-40(5Al-Zn) solders hot-dipped on Cu substrate after various thermal cycles.

was increased since the reaction between Al, Zn-rich and IMC layer might enhance the bonding strength between IMC layer and solder. In addition, due to the higher melting point of the alloy with higher x value, the dipping temperature was different for the solders used (250°C for $x = 5,9$; 300°C for $x = 20,30$; 350°C for $x = 40$). The CTE mismatch due to rapid cooling in solidification of Sn-Zn-Al solder with higher 5Al-Zn contents (20, 30, and 40 wt%) induces residual stress at the interface between Al, Zn-rich and Sn-rich, and near IMC/solder. It can explain that the adhesion strength of $(100 - x)$Sn-x(5Al-Zn) solder with higher x value was lower than that of the lower x one. However, the stress

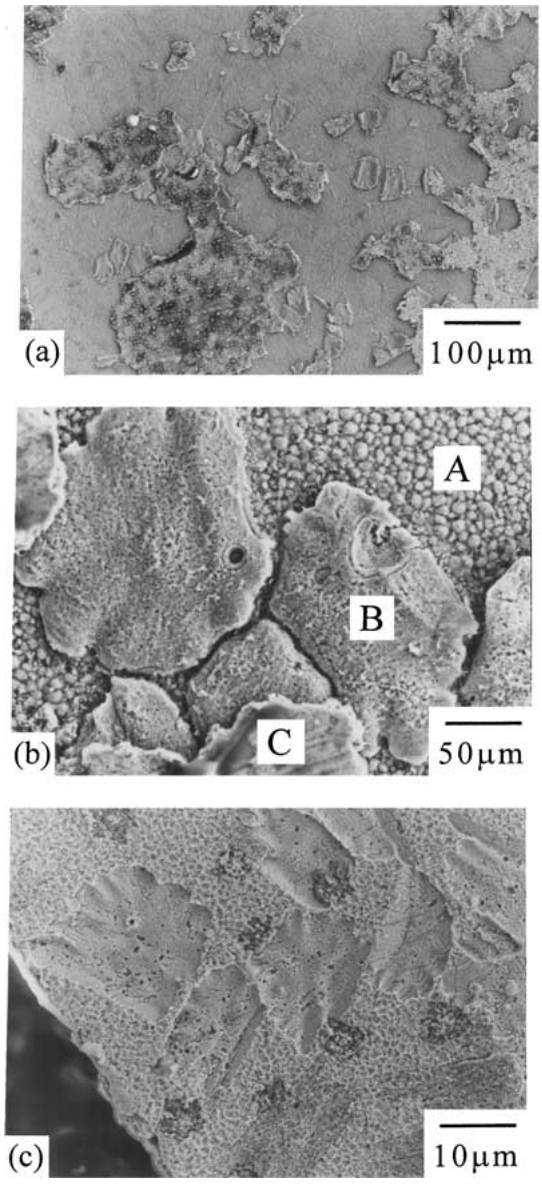

Figure 6 The micrographs of fracture surface at (a) low magnification and (b) high magnification for the 70Sn-30(5Al-Zn) solder after 40 thermal cycles while (c) Al stud site.

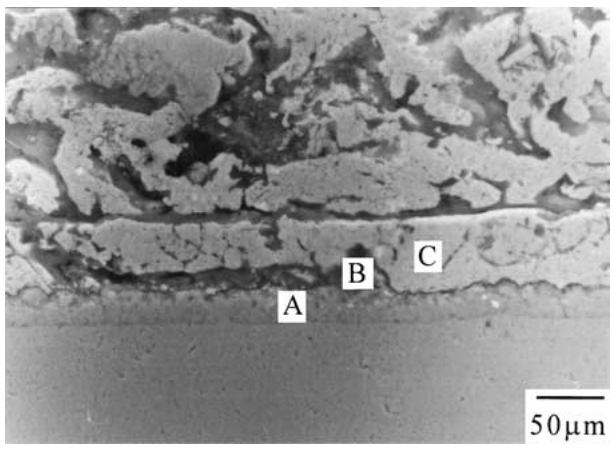

Figure 7 Cross-sectional SEM micrograph of 70Sn-30(5Al-Zn) after 40 thermal cycles.

relaxation seems to occur after thermal cycling in those Sn-Zn-Al solders with higher 5Al-Zn contents. The reaction between Al, Zn-rich (A area) and IMC layer (B area) causes the stress relaxation, which was induced

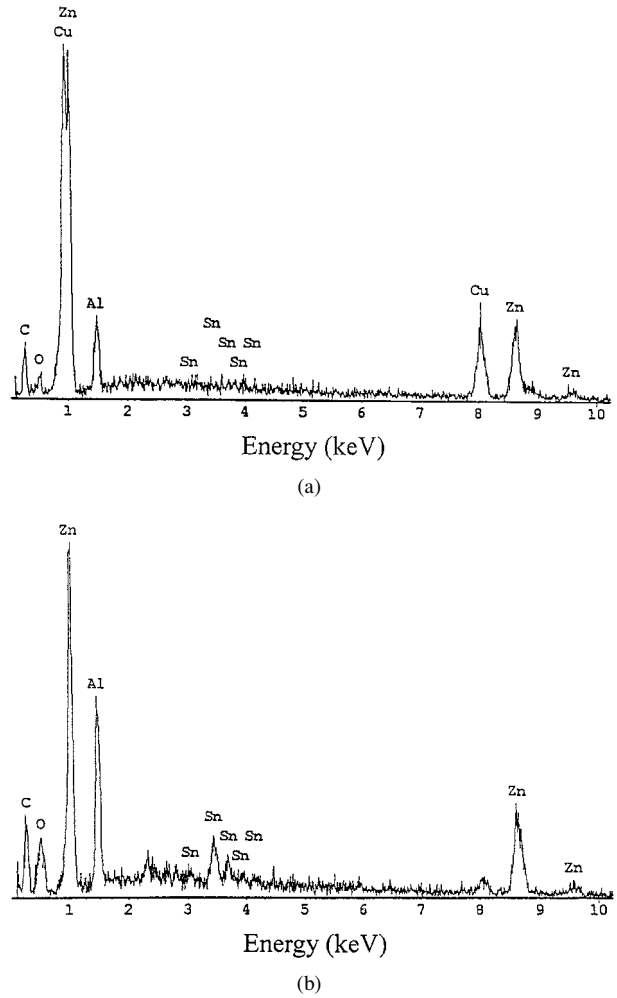

Figure 8 EDS analyses of (a) A and (b) B areas in Fig. 7.

in rapid cooling strengthening the adhesion bonding as measured by the pull-off test. The fracture was found at the Al, Zn-rich/Sn-rich area instead of IMC/Sn-rich interface.

Yu *et al*. [10] reported that the Al and Zn diffuse faster than Cu, also the free energies of Cu_9Al_4 and Cu_5Zn_8 are much lower than that of Cu_3Sn and Cu_6Sn_5 and would be more stable, which explains the formation of Cu_9Al_4 and Cu_5Zn_8 instead of Cu-Sn compounds in 91Sn-9(5Al-Zn) solder system. More Al, Zn-rich area adjacent to the Cu substrate of the solder with higher 5Al-Zn content results in the thicker IMC layer and the lower adhesion strength of solder with higher 5Al-Zn contents, especially after long time heating [8]. In addition, the stress at interfaces of the Al, Zn-rich area with higher CTE value and lower CTE value such as Sn-rich and IMC layer would be released after thermal cycles.

The increase of bonding strength between IMC and Cu made the fracture occur at Al, Zn-rich/solder interface like B region as revealed in Fig. 6b. The Cu/Al, Zn rich interface was strengthened due to the intermetallic formation.

4. Conclusion

For the $(100 - x)$Sn-x(5Al-Zn) solder with the x value increased up to 40 wt%, the adhesion strength decreased from 11.8 ± 1.5 to 3.3 ± 0.9 MPa. As thermal cycling was up to 40, the adhesion strength of 95Sn-5(5Al-Zn)

and 91Sn-9(5Al-Zn) decreased from 11.2 ± 1.7 to 8.2 ± 1.3, 7.6 ± 0.7 to 5.0 ± 0.8 MPa, respectively. However, the adhesion strength of 80Sn-20(5Al-Zn), 70Sn-30(5Al-Zn) and 60Sn-40(5Al-Zn) solders increased from 5.7 ± 1.7 to 13.3 ± 1.9 MPa, 4.8 ± 2.0 to 12.2 ± 1.8 MPa, and 3.3 ± 1.5 to 16.2 ± 1.2 MPa, respectively, when the thermal cycling were up to 40.

Comparing the fracture surface of $(100 - x)$Sn-x (5Al-Zn) solders with $x = 20$, 30 and 40 that as-dipped and after 40 thermal cycles, different fracture regions were found in SEM micrographs. The Al, Zn-rich/Sn-rich area was found on the fracture surface of solders with 5Al-Zn contents of 20, 30 and 40 wt% after thermal cycling and then pull-off.

Acknowledgement

This work was supported by the National Science Council, Taiwan, the Republic of China under Contract No. NSC87-EPA-P-006-002, which is gratefully acknowledged.

References

1. J. H. LAU, "Chip on Board Technologies for Multichip Modules" (International Thomson Publishing Company, New York, 1994) chap. 1.
2. M. PECHT, "Handbook of Electronic Package Design" (Marcel Decker, New York, 1991) chap. 1.
3. D. R. FREAR, D. GRIVAS and J. W. MORRIS, *J. Electron. Mater.* **17**(2) (1988) 171.
4. C. S. CHANG, A. OSCILOWSKI and R. BRACKAN, *IEEE Circuits and Devices Magazine* **14**(2) (1998) 45.
5. D. R. FREAR, W. B. JONES and K. R. KINSMAN, in "Solder Mechanics," 1st ed. (Santa Fe, New Maxico, 1990) p. 206.
6. R. YENAWINE, M. WOLVERTON, A. BURKETT, B. WALLER, B. RUSSEL and D. SPRITZ, in Proc. 11th Naval Weapons Electronics Manufacturing Seminar, China Lake, CA, 1987, p. 339.
7. Y. KARIYA and M. OTSUKA, *J. Electron. Mater.* **27**(7) (1998) 866.
8. S. P. YU, M. H. HON, H. C. WANG and M. C. WANG, *J. Miner. Metals and Mater. (JOM)* **52**(6) (2000) 38.
9. S. P. YU, M. C. WANG and M. H. HON, *J. Electron. Mater.* **29** (2000) 237.
10. S. P. YU, M. H. HON and M. C. WANG, *J. Mater. Res.* **16**(1) (2001) 76.
11. S. P. YU, C. L. LIAO, M. H. HON and M. C. WANG, *J. Mater. Sci.* **35** (2000) 4217.
12. S. P. YU, S. J. LIN, M. H. HON and M. C. WANG, *J.M.S.-Mater. in Electron.* **11** (2000) 461.
13. T. TAKEMOTO, A. MATSUNAWA and M. TAKAHASHI, *J. Mater. Sci.* **32** (1997) 4077.
14. T. E. WONG, L. A. KACHATORIAN and B. D. TIERNEY, *Trans. of ASME, J. Electron. Packaging* **119** (1997) 171.
15. D. R. LIU and Y. H. PAO, *J. Electron. Mater.* **26**(9) (1997) 1058.
16. C. G. SCHMIDT, J. W. SIMONS, C. H. KANAZAWA and D. C. ERLICH, *IEEE Trans. on Components, Packaging, and Manufacturing Technology A* **18** (1995) 611.
17. A. R. SYED, *Trans. of ASME, J. Electron. Packaging* **117** (1995) 116.
18. S. M. LEE and K. W. LEE, *Jpn. J. Appl. Phys.* **35** (1996) L1515.
19. R. G. ROSS, JR. and L. C. WEN, *Trans. of ASME, J. Electron. Packaging* **116** (1994) 69.
20. G. W. C. KAYE and T. H. LABY, "Tables of Physical and Chemical Constants and Some Mathematical Functions," 13th ed. (Butterworth & Co. Ltd., 1966) p. 55.

Received 27 June 2000
and accepted 3 August 2001